JP1.9 A QUANTITATIVE COMPARISON OF MM5 CLOUD FORECASTS AND GOES CLOUD ANALYSES

Michael A. Kelly, Randall J. Alliss*, Mary Ellen Craddock, Jerry C. Lefever
Litton-TASC, Chantilly, Virginia

1. INTRODUCTION

In order to mitigate the influence of adverse weather, it has become routine for government and civil organizations to rely on Numerical Weather Prediction (NWP) models to make operational decisions (Roebber and Bosart, 1996). But NWP cloud simulations are fraught with challenges that limit their accuracy. No routine observations of cloud water and cloud ice are taken, therefore NWP models are usually initialized with zero cloud condensate or with condensate mass distributions obtained from earlier runs. Microphysics cloud parameterizations are usually validated based on case studies of winter storm events (*e.g.* Schultz, 1995). But how well do models forecast clouds on a day-to-day basis, particularly when forcing is weak or terrain-dependent? Our study answers this by statistically comparing cloud forecasts from a high-resolution mesoscale model with cloud analyses from a meteorological satellite.

2. MODEL

The model used for this experiment is the fifth generation of the Pennsylvania State University/National Center for Atmospheric Research (NCAR) Mesoscale Model (Version 3) (MM5). It is a nonhydrostatic, compressible mesoscale modeling system with many options for grid configurations and physics parameterizations. A recent description of the model options can be found in Dudhia (2000).

The model was configured with 23 vertical σ layers, specified so as to give higher resolution near the surface and lower resolution near the model top at 100 mb. As shown in Figure 1, domain 4 (90×90 points) and domain 3 (55×55 points) have 4-km and 12-km horizontal spacing, respectively. Model output-cloud analysis comparisons were confined to these two nests. The microphysics scheme selected for this study simulates precipitation events with accuracy comparable to, but executes faster than, more sophisticated research-grade schemes (Schultz 1995). The Schultz microphysics parameterization has prognostic equations for 5 water species (cloud liquid, cloud ice, rain, snow, precipitation ice). The small horizontal grid spacing of domain 4 requires that convection be explicitly resolved for that nest. The convection scheme for the outer domains follows Grell (1993). The radiation scheme used for this study explicitly models the interaction between radiation and cloud species (Dudhia 1989). The Hong-Pan boundary-layer parameterization (Hong and Pan, 1996), which models non-local counter-gradient diffusion, represents the boundary layer for these runs.

Corresponding author: Dr. Randall J. Alliss, TASC, 4801 Stonecroft Blvd., Chantilly, VA 20151; e-mail: rjalliss@tasc.com

3. SATELLITE ANALYSES

Satellite analyses for this study were derived from a multi-spectral cloud-detection algorithm (Alliss *et. al*., 2000) applied to Geostationary Operational Environment Satellite (GOES) 8, 9, and 10 imager data. For each satellite pixel and channel, the difference between the GOES brightness temperature and the clear-sky background (CSB) is computed. Season- and location-dependent difference thresholds are then applied to each difference. If the pixel passes the time-dependent combination of threshold tests, then it is tentatively labeled as cloudy. A series of tests are then applied to eliminate false-cloud signatures, which result due to soil emissivity (soil type), snow cover, or terrain. This defines the composite cloud determination for that pixel and time. The horizontal resolution of this cloud analysis is 4 km. The main weakness of this algorithm is found during the transition between day and night (night and day) when the CSB tends to be too warm (cold). This can lead to an over / underestimate in clouds of up to 5 %.

4. PROCEDURE

The model was initialized with 00-UTC or 12-UTC analyses and run for 24 h twice per day during February 2000. Initial and boundary conditions were derived from analyses and forecasts, respectively, from the National Centers for Environmental Prediction (NCEP) ETA model. No assimilation or warm-start procedures were adopted for this initial experiment. The cloud water and cloud ice fields were therefore initialized to zero. All model output fields were written out hourly.

A statistical analysis was conducted as follows. The cloud optical depth for MM5 simulations was computed from

$$\tau = a_l LWP + a_i IWP \,, \qquad (1)$$

where LWP and IWP are the liquid and ice water paths in units of kg m^{-2}. The absorption coefficients for cloud water a_l and cloud ice a_i were specified as 150 m^2 kg^{-1} and 50 m^2 kg^{-1} based on Stephens (1978). Following Manning and Davis (1997), rain, snow, and precipitating ice species were ignored in the calculation of cloud optical depth, because these fields generally occur beneath layers that have considerable cloud ice and water.

The nominal sensitivity of the GOES imager is τ = 0.1. That is, the GOES imager senses approximately 50% of the clouds with τ = 0.1 (Menzel, *et. al*., 1992). To be consistent, MM5 grid columns with $\tau \geq 0.1$ were designated as "cloudy" grid columns.

MM5 and GOES use lambert conformal map projection and latitude-longitude grid, respectively, and so the MM5 and GOES grids are offset. Each grid column from MM5 was therefore compared with the GOES pixel with which it shared the most common area. Two statistical measures were then calculated based on a direct pixel-to-pixel comparison. The bias B is defined as

$$B \equiv \bar{f} - \bar{a}\,, \qquad (2)$$

where $\bar{f}$ and $\bar{a}$ are the mean number of grid cells forecast and observed to be cloudy, respectively. For our definition of bias, a perfect score is zero; a positive bias indicates more cloud was forecast than observed. The threat score T is defined as

$$T \equiv \frac{C - \varepsilon}{F + O - C - \varepsilon}\,, \qquad (3)$$

where C is the total number of grid boxes correctly forecast to be cloudy, F is the number grid boxes forecast to be cloudy, O is the number of grid boxes observed to be cloudy, and ε is the expectation which is given by $F*O/N$. N is the total number of grid columns. The threat score rewards successful forecasts of rare events, but penalizes for over-forecasting. A perfect score is one, while zero signals no skill.

5. RESULTS

The model exhibited little skill during the first six hours of the simulations. During this initial period, the probability that cloud fields simulated by MM5 were observed was approximately 55%. The poor performance resulted from cloud condensate fields that were initialized to zero. During this initial "spinup" period, the model generated cloud fields that were not necessarily realistic. A large literature exists on the subject of model initialization (*e.g*. Gustafsson *et al*., 1997).

Figure 2 shows the probability that cloud was observed, as a function of MM5 cloud optical depth. The left (right) panel gives the result obtained using 6-h cloud optical depth forecasts computed from the 00-UTC (12-UTC) MM5 runs. The probabilities were computed using 10,000 bins for cloud optical depths in the range between 0 and 10.

For τ > 0.1, the probability of cloud (POC) was generally greater than 50%. For τ >1, the POC exceeded 80% for the 12-UTC runs, while the POC hovered between 50% and 60% for the 00-UTC runs. This difference relates to the daily cycle of cloud forcing. The forcing tends to be stronger during the day, and so the 12-UTC runs generated realistic cloud fields within a relatively short period. At night, the forcing is weaker and more terrain-dependent, and so forecast cloud fields were not always realistic.

This assertion is supported by the left panel of Figure 3, which shows that the 00-UTC 18-h cloud forecasts were much more accurate than the 00-UTC 6-h cloud forecasts. The cloud fields self-corrected due to the much stronger forcing that occurs during the day. In this case, the POC for τ > 3 was 70% or more. Note, however, that the vast majority of clouds simulated by MM5 had optical depths less than one.

Consider now the right panel of Fig. 3. The accuracy of cloud forecasts was very good (75 %) for clouds with τ > 3, but the POC for thinner clouds decreased. During the MM5 12-UTC simulations, the cloud fraction increased steadily from zero to 0.595 at 24 h into the simulation. The GOES cloud analyses indicate a moderate diurnal cycle during February 2000 with clouds over domain 4 decreasing from a maximum cloud fraction of 0.41 at 21 UTC to a minimum of 0.31 at 10 UTC. The model lacks a realistic diurnal cycle of clouds, which explains the reduced POC for thin cloud in the right panel. The thick clouds were usually produced by strong dynamic forcing, and so were less affected by the diurnal cycle.

The model's poor performance suggested that we should test different microphysics schemes to determine which performs best for this region. We calculated forecast statistics for the simple ice, mixed phase, Goddard GSFC, and Reisner microphysics parameterization options of MM5. The simple ice scheme includes cloud ice, cloud water, rain, and snow, but excludes supercooled water. The mixed-phase scheme allows liquid and ice to coexist, but lacks graupel and riming processes. The Goddard microphysics scheme (Tao *et al*., 1993) includes a prognostic equation for graupel. The Reisner graupel scheme is based on the mixed phase scheme, but adds predictive equations for graupel and ice number. Details of these

schemes (except Goddard) may be found in Reisner *et al*. (1998). Due to the large amount of processing required, we performed 18-h simulations twice per day for the first week of February only.

Figure 4 shows that persistence beats the model during the first 5 hours. This is not surprising given that the model must spin up its cloud fields during this initial period. The Reisner scheme achieved the highest threat score (0.4) at 9 h, but fell thereafter so that it beat only persistence after 13 h. The Schultz scheme performed best between 12 h and 16 h, but its score was approximately equivalent with those of simple ice, mixed layer and Goddard during the last two hours of the simulation.

Figure 5, which shows the bias for each microphysics parameterization as a function of forecast hour, gives insight into the behavior of the schemes in Fig. 4. The bias was initially negative for each scheme's runs (with cloud condensate initialized to zero), but it increased until the forecasts for each scheme significantly overestimated cloud. During the initial four hours, the cloud field adjusted to a bias that was steady for the next 4-6 hours. The bias then increased at a rate of 10 % h^{-1} for three hours, after which the trend steadied.

Although runs with the Schultz scheme followed the pattern just described, its bias remained negative throughout much of the forecast period. This tendency resulted in greater skill between 12 h and 16 h. After its bias increased to 0.2 (equivalent with the other schemes), runs with the Schultz scheme displayed no greater forecast skill than other runs. Similarly, runs using the Reisner scheme displayed the most skill between 5 h and 11 h, after which time the bias passed through 0.2. The forecast performance of the various schemes therefore depended on their cloud biases as a function of forecast hour.

Manning and Davis (1997) found similar results in their verification of WISP94 MM5 cloud forecasts. Real-time forecasts were generated twice per day with MM5 configured to use the Reisner microphysics parameterization on grids with 60-km and 20-km spacing. Manning and Davis attributed the cloudy bias in MM5 to the use of Fletcher's (1962) formula for ice nuclei number concentration by the Reisner scheme, to a mid-level cold bias induced by the application of a radiative temperature tendency, and a low-level cold bias induced by excessive moisture availability at the surface. By using the Schultz scheme and a detailed radiative transfer parameterization, our experimental setup should have removed the first two factors cited by Manning and Davis. Further work will be required to verify that the mid-level cold bias has been removed and to quantify the sensitivity of each scheme to surface moisture availability.

6. SUMMARY AND CONCLUSIONS

A set of NWP forecasts were generated twice per day during February 2000 and evaluated for forecast accuracy. The results were decidedly mixed. Although the POC was generally greater than 70 % for optically thick clouds, forecast accuracy was found to depend on the length of the forecast and the time of day in which the forecast was initialized. Cloud forecasts tended to be highly accurate when the dynamical forcing was strong. Every MM5 microphysics parameterization tested was found to generate more clouds than observed. More work is required to isolate the cause of the cloudy bias in MM5.

7. REFERENCES

Alliss, R. J., M. E. Loftus, D. Apling, J. Lefever, 2000: The development of cloud retrieval algorithms applied to GOES digital data. Preprints, *10th Conference on Satellite Meteorology*, Long Beach, CA, AMS, 330-333.

Dudhia, J., 1989: Numerical study of convection observed during the winter monsoon experiment using a mesoscale two-dimensional model. *J. Atmos. Sci*., **46**, 3077-3107.

Dudhia, J: 2000: Recent developments and plans for MM5. Preprints, *10th PSU/NCAR Mesoscale Model Users' Workshop*, Boulder, CO, NCAR/MMM, 6-8.

Fletcher, N. H., 1962: *Physics of Rain Clouds*. Cambridge University Press, 386 pp.

Grell, G. A., 1993: Prognostic evaluation of assumptions used by cumulus parameterizations. *Mon. Wea. Rev*., **121**, 764-787.

Gustafsson, N., P. Lönnberg, J. Pailleux, 1997: Data assimilation for high-resolution limited-area models. *J. Met. Soc. Jap*, **75**, 367-382.

Hong, S.-Y., H.-L. Pan, 1996: Nonlocal boundary layer vertical diffusion in a medium-range forecast model. *Mon. Wea. Rev*., **124**, 2322-2339.

Manning, K. W. and C. A. Davis, 1997: Verification and Sensitivity Experiments for WISP94. *Wea Forecasting*, **12,** 719-735.

Menzel, W.P., D.P. Wylie, and K. I. Strabala, 1992: Seasonal and diurnal changes in cirrus clouds as seen in four years of observations with VAS., *J. Appl. Meteor.,* **42**,2333-2349.

Reisner, J., R. M. Rasmussen, and R. T. Bruintjes, 1998: Explicit forecasting of supercooled liquid water in winter storms using the MM5 mesoscale model. *Quart J. Roy. Met. Soc*., **124**, 1019-1105.

Roebber, P. J. and L. F. Bosart, 1996: The complex relationship between forecast skill and forecast value: a real-world analysis. *Wea. Forecasting*, **11**, 544-559

Schultz, P., 1995: An explicit cloud physics parameterization for operational numerical weather prediction. *Mon Wea. Rev*., **123**, 1331-3343.

Stephens, G. L., 1978: Radiation Profiles in Extended Water Clouds. II: Parameterization Schemes. *J. Atmos Sci*., **35**, 2123-2132.

Tao, W.-K., and J. Simpson: 1993: Goddard Cumulus Ensemble Model. Part I: Model description. *TAO*, **4**, 35-72.

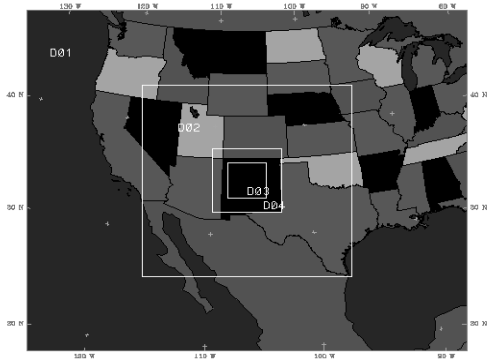

Figure 1: The domain setup for the MM5 February runs. Domains 1, 2, 3, and 4 have 108-, 36-, 12-, and 4-km grid spacing, respectively.

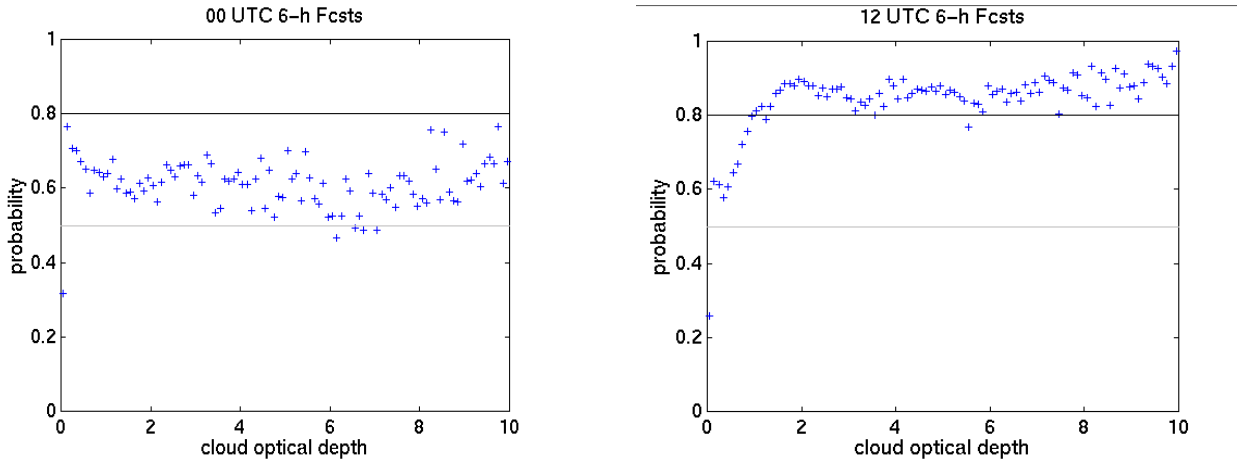

Figure 2: The probability of cloud observed in the GOES analysis as a function of cloud optical depth computed from MM5 6-h cloud water and cloud ice fields. The left and right panels are for 00 UTC and 12 UTC February simulations, respectively.

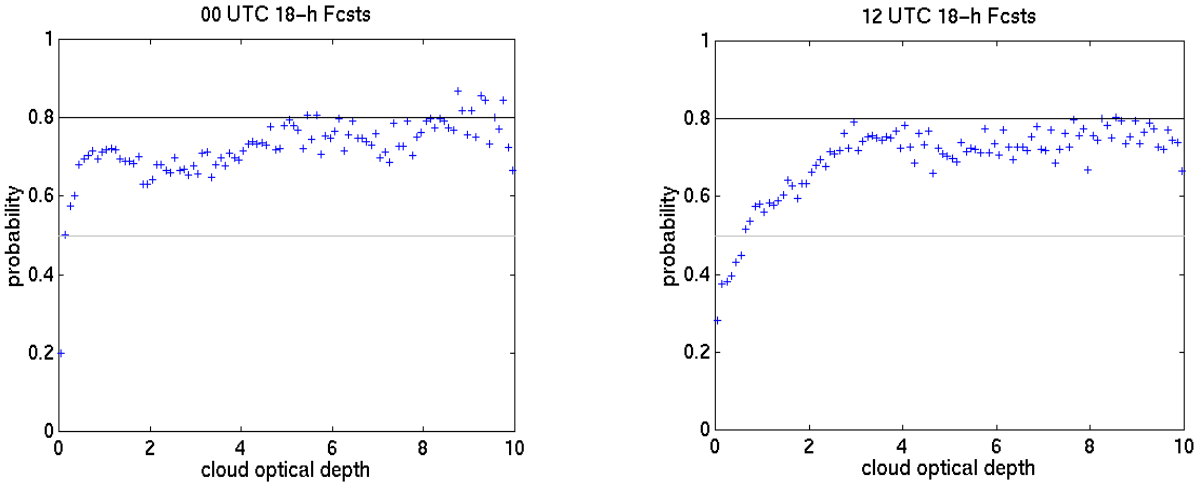

Figure 3: Same as Figure 2, except cloud optical depth is computed from MM5 18-h cloud water and ice.

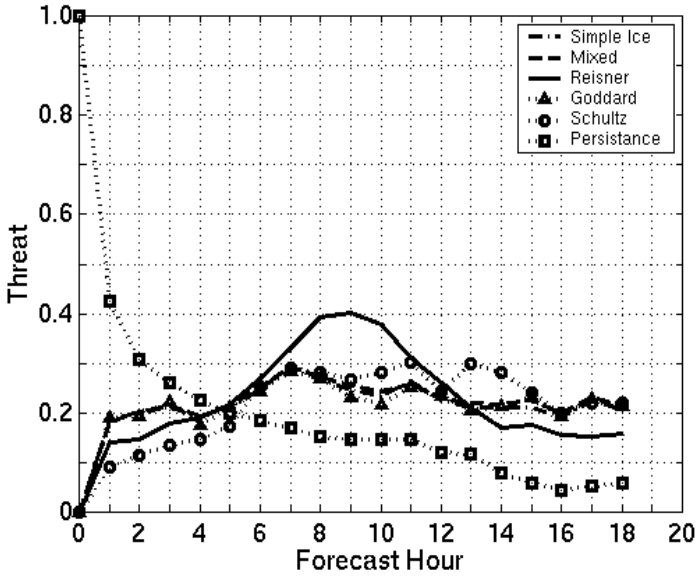

Figure 4: The threat score as a function of forecast hour for 5 microphysical schemes and for persistence. The dashed-dotted curve denotes the simple ice scheme, the dashed curve denotes the mixed phase scheme, the solid curve denotes the Reisner scheme, the curve with triangles denotes the Goddard scheme, the curve with circles denotes the Schultz scheme, and the curve with squares denotes persistence.

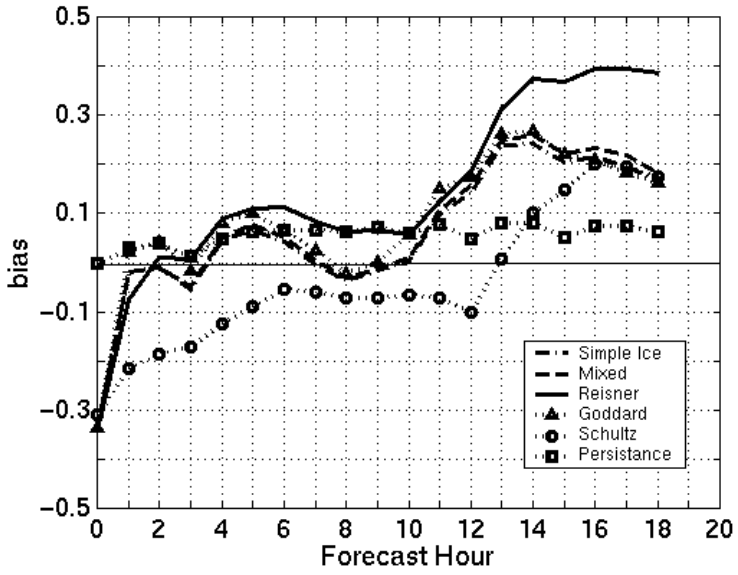

Figure 5: The bias (Eqn 2) as a function of forecast hour for 5 microphysical schemes and for persistence. The dashed-dotted curve denotes the simple ice scheme, the dashed curve denotes the mixed phase scheme, the solid curve denotes the Reisner scheme, the curve with triangles denotes the Goddard scheme, the curve with circles denotes the Schultz scheme, and the curve with squares denotes persistence.